STRAIN RELIEF AND Pd ISLAND SHAPE EVOLUTION ON THE PALLADIUM AND PALLADIUM HYDRIDE (100) SURFACE

S. V. Kolesnikov[*], *A. L. Klavsyuk*, *A. M. Saletsky*

Lomonosov Moscow State University
119991, Moscow, Russia

The mesoscopic relaxation of small Pd islands on $Pd(100)$ and $PdH(100)$ surfaces is investigated on the atomic scale by performing molecular statics calculations. A strong strain and stress inhomogeneity in islands and topmost layers of the substrate is revealed. An unusual size dependence of the shape of islands is discovered.

1. INTRODUCTION

The mesoscopic relaxation of small islands and the underlying substrate atoms can play a crucial role in thin film growth. Numerous interesting phenomena are closely related to relaxation effects. A fast island decay was discovered in homoepitaxial growth [1]. In-plane lattice oscillations were observed during the heteroepitaxy and homoepitaxy [2]. Experiments on atom movement on and near islands have shown the existence of empty zones near the edges of islands [3, 4]. Phenomena such as borrowing of small clusters [5] and unusual magnetic [6] and electronic properties [7] of surfaces and nanostructures cannot be completely understood without taking the effects of mesoscopic relaxation into account. From this standpoint, the understanding of mesoscopic relaxation is of great importance for developing nanoelectronic and advanced magnetic devices.

During the last two decades, the mesoscopic relaxation of thin films and substrate layers was investigated for many metal and semiconductor systems like $Ni/W(110)$ [8], $Ag/Pt(111)$ [9], $Fe/Pd(100)$ [10], $Ge/Si(100)$ [11], etc. The most significant feature of these systems is the insufficiency of the classical theory based on the lattice mismatch between the film and the substrate. Theoretical works using the tight-binding (TB) approximation [12, 13], the embedded atoms method [14, 15], and the density functional theory (DFT) [16, 17] showed that the accurate description of strain relaxation requires going down to the atomic level.

Following theoretical works [12, 13], we note some

general peculiarities of mesoscopic relaxation: (i) the mesoscopic misfit exists in both homoepitaxial and heteroepitaxial systems and depends on the size of nanostructures, (ii) small islands and the surface under these islands are not flat due to the strain relaxation, and (iii) the mesoscopic mismatch leads to a strongly inhomogeneous stress distribution in the islands and in the substrate. Recently, these statements were directly proved in surface X-ray diffraction (SXRD) experiment in [18, 19] for $Co/Cu(100)$. However, some principal questions like the effect of impurity atoms on strain relaxation are not yet totally clear.

To investigate mesoscopic relaxation, we have chosen $Pd/Pd(100)$ and $Pd/PdH(100)$ for several reasons. The macroscopic misfit between palladium and palladium hydride is not too large ($\approx 5.6\%$) and is close to the macroscopic misfit in the $Co/Cu(100)$ system ($\approx 2\%$) investigated in Ref. [12]. On the other hand, the interaction between palladium and hydrogen atoms is relatively weak and we can consider the strain relaxation of the Pd and H sublattices independently. Moreover, this investigation may be helpful for understanding adsorption on the palladium hydride surfaces.

This paper has the following structure. In Sec. 2, the computational method is described. In Sec. 3, we present the results of theoretical studies of strain relaxations in $Pd/Pd(100)$ and $Pd/PdH(100)$ systems. Finally, in Sec. 4, we conclude the paper with general remarks.

2. COMPUTATIONAL METHOD

To investigate the structural properties of $Pd(100)$ and $PdH(100)$ surfaces, we use the Molecular Statics

---

[*]E-mail: kolesnikov@physics.msu.ru

(MS) method. We can describe Pd and H atoms as classical particles interacting via interatomic potentials. In this paper, interatomic potentials are formulated in the second moment of the TB approximation [20]. In the TB approximation, the attractive term E_B^i (band energy) contains the many-body interaction. The repulsive part E_R^i is described by pair interactions (Born–Mayer form). The cohesive energy E_C is the sum of the band energy and the repulsive part,

$$E_C = \sum_i \left(E_R^i + E_B^i \right), \qquad (1)$$

$$E_B^i = -\left\{ \sum_j \xi_{\alpha\beta}^2 \exp\left[-2q_{\alpha\beta} \left(\frac{r_{ij}}{r_0^{\alpha\beta}} - 1 \right) \right] \right\}^{1/2}, \quad (2)$$

$$E_R^i = \sum_j A_{\alpha\beta}^0 \exp\left[-p_{\alpha\beta} \left(\frac{r_{ij}}{r_0^{\alpha\beta}} - 1 \right) \right], \qquad (3)$$

where r_{ij} is the distance between atoms i and j, α and β are types of atoms, $\xi_{\alpha\beta}$ is an effective hopping integral, $p_{\alpha\beta}$ and $q_{\alpha\beta}$ describe the decay of the interaction strength with the distance between atoms, and $r_0^{\alpha\beta}$ and $A_{\alpha\beta}^0$ are adjustable parameters of the interatomic interaction. The interatomic potentials reproduce the bulk properties of Pd and PdH crystals, structural and energetic properties of clean and H-covered Pd(100) and Pd(110) surfaces, and phonon spectra in the bulk and at the surface of Pd–H systems [21–24]. This approach was recently applied to the investigation of the effect of hydrogen on the surface relaxation of Pd(100), Rh(100), and Ag(100) [25]. We note that the Hamiltonian underlying the energy expressions in Eqs. (1), (2), and (3) describes the essential physics governing cohesion in many solids [26].

To demonstrate that TB potentials can describe the relaxation of small Pd islands on PdH(100) surface with good accuracy, we calculate the first Pd–Pd bond length r in the palladium dimer and in a Pd$_4$ square island on the PdH(100) surface. We compare these results with the calculations by the VASP code [27–29] based on the DFT. The local density approximation (LDA) for the exchange-correlation functional has been applied. To simplify the comparison of TB and DFT results, we perform the calculations for identical small cells in both cases. The slab consists of four layers with 18 Pd atoms and 18 H atoms in each layer. Periodic boundary conditions are applied in the surface plane. The palladium dimer (or the Pd$_4$ island) is deposited on the top of the slab. Using the TB approximation and the VASP code, we find the first Pd–Pd

bond length r_2 in the palladium dimer on PdH(100) surface as $r_2^{TB} = 2.777$ Å and $r_2^{DFT} = 2.757$ Å. For the first Pd–Pd bond length r_4 in the Pd$_4$ square island on the PdH(100) surface, the calculations based on the TB approximation and the DFT also yield very close results: $r_4^{TB} = 2.764$ Å and $r_4^{DFT} = 2.753$ Å. These results indicate that the interatomic potentials in (1), (2), and (3) give a good description of the relaxation of small palladium islands on the PdH(100) surface.

To determine the hydrostatic stress $P_\sigma = \text{tr}(\sigma_{\alpha\beta})$ in the Pd islands and in the PdH(100) surface layer, we perform calculations of the atomic level stress components [30]:

$$\sigma_{\alpha\beta}(i) = -\frac{1}{\Omega_0} \left[\frac{p_i^\alpha p_i^\beta}{m_i} + \frac{1}{4} \sum_j \left(r_{ij}^\beta f_{ij}^\alpha + r_{ij}^\alpha f_{ij}^\beta \right) \right], \quad (4)$$

where $(\alpha\beta) \equiv (x, y, z)$, m_i and p_i are the mass and momentum of atom i, $\mathbf{f}_{ij}$ is the force acting on atom i due to atom j, and Ω_0 defines the average atomic volume.

The relaxation of the PdH system is computed by means of the MS using the interatomic potentials in the TB approximation, where the positions of Pd and H atoms and the forces $\mathbf{f}_{ij}$ are determined in fully relaxed geometry. The slab consists of nine layers: two bottom layers are fixed and periodic boundary conditions are applied in the surface plane. The cutoff radius for the interatomic potentials is set to 7.0 Å.

3. RESULTS AND DISCUSSIONS

Relaxation of the Pd(100) surface was investigated with the use of interatomic potentials (1), (2), and (3) in Ref. [20]. We therefore start our investigation from the relaxation of clean and Pd-covered PdH(100) surfaces. For the PdH crystal with a NaCl structure, the interlayer distance in the $\langle 100 \rangle$ direction is $d_{bulk}^{PdH} = 2.07$ Å [20]. The hydrostatic stresses for Pd and H atoms calculated with Eq. (4) are $P_\sigma^{Pd} = 0.49$ eV/Å^3 and $P_\sigma^{H} = -0.49$ eV/Å^3. Considering the PdH crystal as a combination of two sublattices, we can conclude that the Pd sublattice is under the tensile and the H sublattice is under the compressive stress, and hence the presence of hydrogen leads to embrittlement of palladium. Relaxation of the topmost layers of the PdH(100) surface leads to the modification of their interlayer distances, the appearance of small spaces between Pd and H layers, and drastic changes in hydrostatic stresses of these layers. The values of relaxation parameters and hydrostatic stresses for clean and Pd-covered PdH(100) surfaces are presented in Tables 1

Table 1. Relaxation at clean and Pd-covered PdH(100) surfaces. The parameters d_0, d_1, d_2, Δ_1, and Δ_2 are illustrated in Fig. 1

Parameters	Clean	Pd-covered
d_0, Å	–	1.91
d_1, Å	1.96	2.03
d_2, Å	2.08	2.08
Δ_1, Å	0.22	0.11
Δ_2, Å	−0.01	0.00

Table 2. Hydrostatic stresses in the topmost layers of clean and Pd-covered PdH(100) surfaces. $P_{\sigma,0}^{\mathrm{Pd}}$ is the hydrostatic stress in the Pd layer, $P_{\sigma,1}^{\mathrm{Pd}}$ and $P_{\sigma,1}^{\mathrm{H}}$ are hydrostatic stresses in the topmost PdH layer, and $P_{\sigma,2}^{\mathrm{Pd}}$ and $P_{\sigma,2}^{\mathrm{H}}$ are hydrostatic stresses in the second PdH layer. In the case of a clean PdH(100) surface, the quantity $P_{\sigma,0}^{\mathrm{Pd}}$ is meaningless

Stress	Clean	Pd-covered
$P_{\sigma,0}^{\mathrm{Pd}}$, eV/Å³	–	0.63
$P_{\sigma,1}^{\mathrm{Pd}}$, eV/Å³	0.51	0.38
$P_{\sigma,2}^{\mathrm{Pd}}$, eV/Å³	0.43	0.48
$P_{\sigma,1}^{\mathrm{H}}$, eV/Å³	−0.03	−0.39
$P_{\sigma,2}^{\mathrm{H}}$, eV/Å³	−0.50	−0.49

and 2. The parameters d_0, d_1, d_2, Δ_1, and Δ_2 are illustrated in Fig. 1. Our results for a clean PdH(100) surface show that hydrogen atoms are pulled significantly from the upper Pd layer, which leads to a drastic decrease in the hydrostatic stress of the topmost hydrogen layer. At the same time, the upper Pd layer is shifted toward the second layer and its hydrostatic stress increases. Changes in the properties of the second PdH layer in comparison with bulk layers are minimal. We next consider the Pd-covered PdH(100). Pulling off the topmost hydrogen layer form a clean PdH(100) surface leads to an increase in the number of "dangling bonds" [22] and, consequently, a decrease in the space d_0 between two topmost palladium layers and an increase ($\approx 20\,\%$) in the hydrostatic stress of the upper Pd layer. We emphasize that the discrepancy between the distance d_0 and the distance between two topmost layers in the Pd(100) surface is less than 0.01 Å. The distances d_1 and Δ_1 become closer to their bulk values, while the hydrostatic stress magnitudes of both Pd and H layers are essentially lower than their bulk values. The parameters of the second PdH layer of Pd-covered PdH(100) surface are quite close to their bulk values. Comparing interlayer distances and hydrostatic stresses in topmost layers of clean and Pd-covered PdH(100) surfaces, we expect strong inhomogeneous strain and stress distributions in the PdH substrate and the Pd island near the edges of islands.

As was emphasized in Ref. [13], the relaxation of edge atoms in mesoscopic islands can become the dominant process leading to the existence of a size-dependent mismatch between the islands and the substrate even in the case of a homogenous system. To illustrate mesoscopic relaxation in homogenous systems, we present the shape and the atomic displacements in the square Pd_{49} island on the Pd(100) surface and in the substrate along the $\langle 110 \rangle$ direction (Fig. 2 a,b). The substrate atoms under the island are pushed down, and
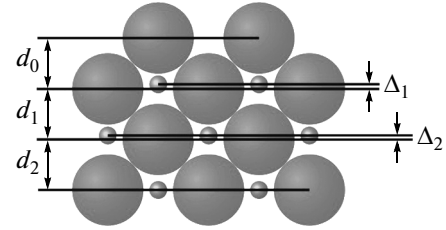

Fig. 1. Schematic side view of the Pd-covered PdH(100) surface showing the interlayer distances d_0, d_1, and d_2, and spaces Δ_1 and Δ_2 between the Pd and H layers. Big spheres represent Pd atoms and small spheres represent H atoms. In the case of a clean PdH(100) surface, the topmost layer is absent and the parameter d_0 is meaningless

the island assumes a tent-like shape. The island locally distorts the surface, which leads to a strongly inhomogeneous stress distribution in the island and in the substrate (see Fig. 2c). The stress in the island is tensile and tends to increase from the edges to the center of the island, while the substrate layer under the island is under compressive stress.

Figure 3 shows the mesoscopic relaxation of the Pd_{49} island on the PdH(100) surface. Comparison of Figs. 2 and 3 yields the following interesting features. The maximal displacement of Pd substrate atoms on the PdH(100) surface is twice that on the Pd(100) surface. At the same time, the displacements of hydrogen atoms are even greater than the displacements of palladium atoms. The space between Pd and H layers under the island decreases and approaches the value Δ_1 for the Pd-covered PdH(100) surface. Increasing the topmost Pd layer distortion leads to a stronger inhomo-
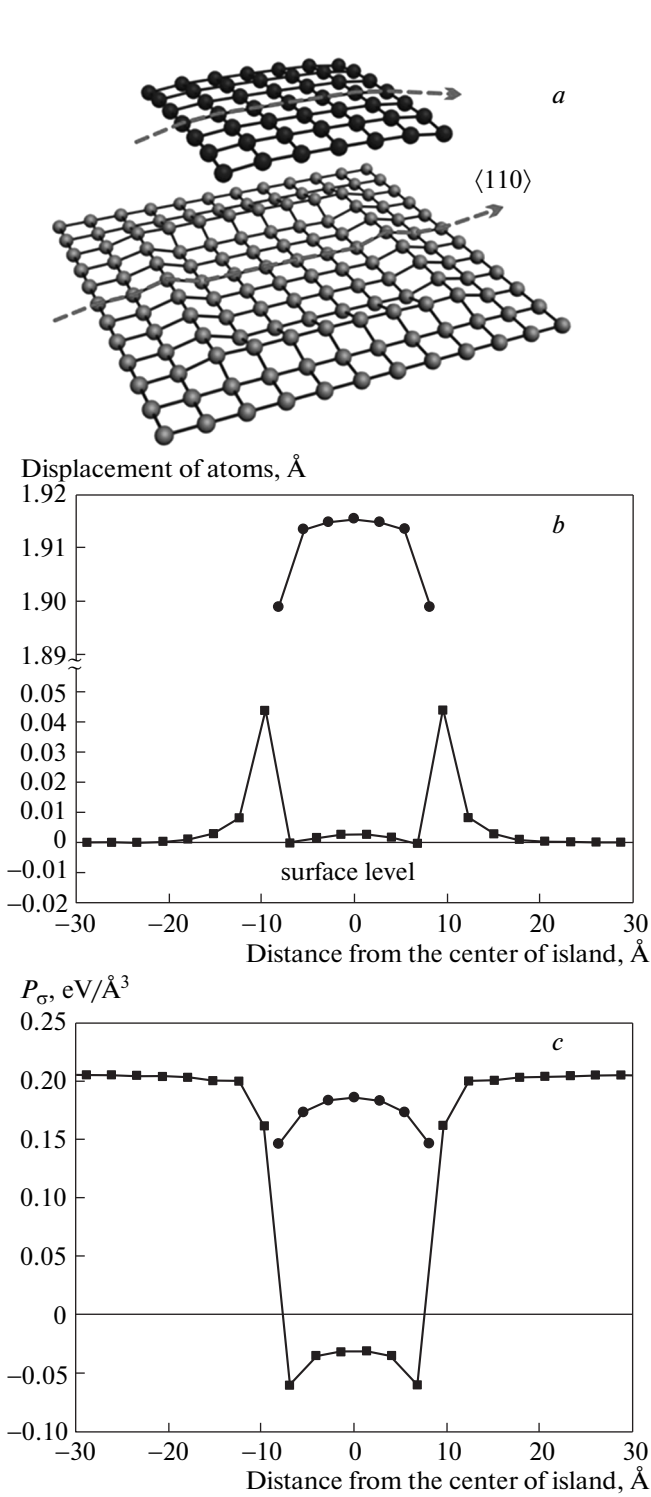
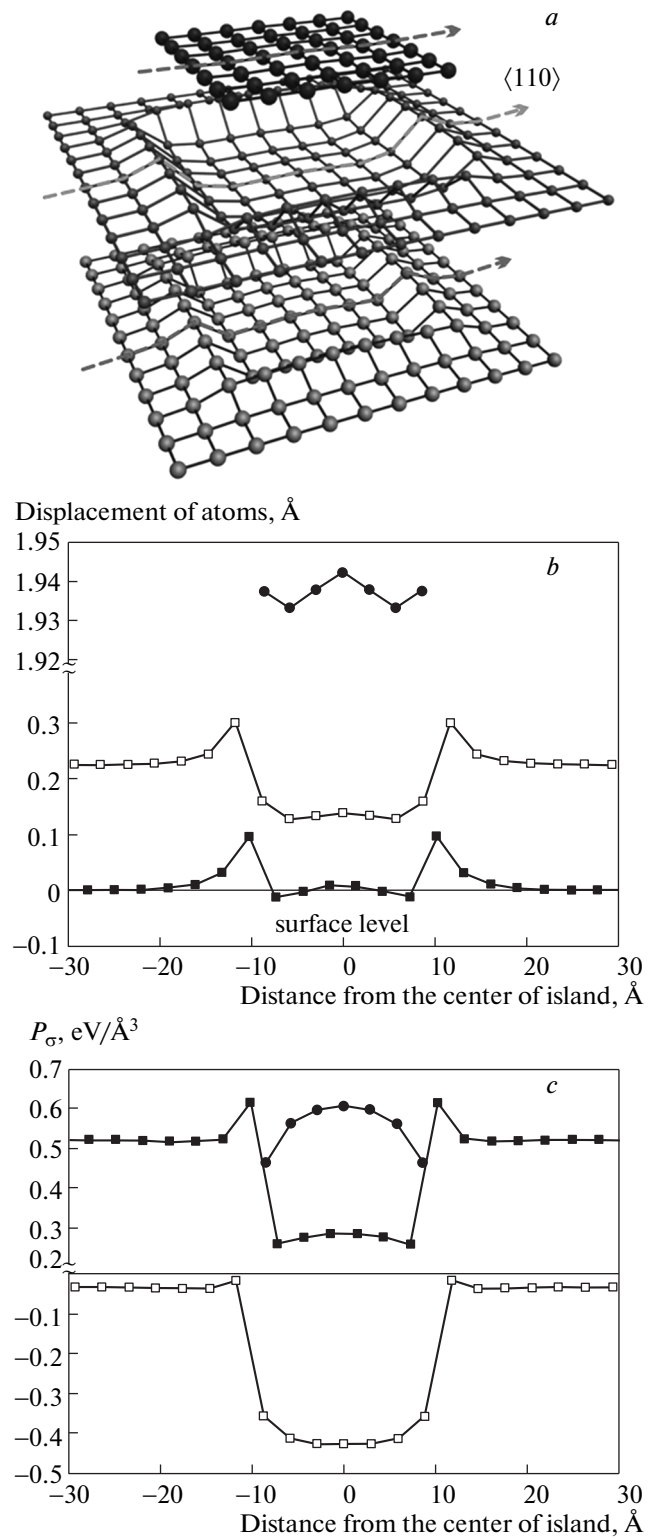Displacement of atoms, Å

P_σ, eV/Å³

Fig. 2. The Pd_{49} island on a $Pd(100)$ surface and the topmost layer under the island: (a) the shape of the island and the substrate layer, (b) the vertical displacement of atoms in the $\langle 110 \rangle$ direction, (c) the hydrostatic stress

Displacement of atoms, Å

P_σ, eV/Å³

Fig. 3. The Pd_{49} island on a $PdH(100)$ surface and the topmost layer under the island: (a) the shape of the island and the substrate layer, (b) the vertical displacement of atoms in the $\langle 110 \rangle$ direction, (c) the hydrostatic stress. Big spheres represent Pd atoms and small spheres represent H atoms
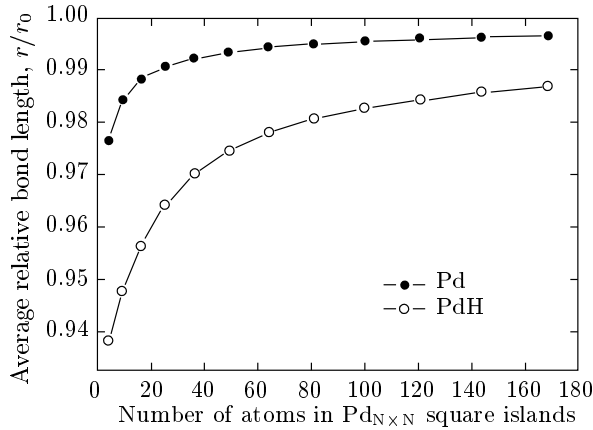
Fig. 4. The average relative Pd–Pd bond length in the single-layer square palladium islands on Pd(100) and PdH(100) surfaces. r is the average first bond length in Pd islands and r_0 is the first Pd–Pd bond length in Pd (2.75 Å) and PdH (2.93 Å)

Fig. 5. The average relative hydrostatic stress in single-layer square palladium islands on Pd(100) and PdH(100) surfaces. $\langle P_\sigma \rangle$ is the average hydrostatic stress in the island and $P_{\sigma,0}$ is the hydrostatic stress in the Pd layer. In the case of the PdH(100) surface, $P_{\sigma,0} = P_{\sigma,0}^{\mathsf{Pd}} = 0.63$ eV/Å^3, and in the case of the Pd(100) surface, $P_{\sigma,0} = 0.21$ eV/Å^3

geneity of stress distribution under the island. But in contrast to the Pd(100) surface, the substrate Pd layer under the island is still under tensile stress, which is compensated by the high compressive stress of the hydrogen layer (Fig. 3c). The main cause of the increase in the strain and stress inhomogeneity of the topmost substrate layer is the appearance of a macroscopic misfit between palladium hydride and clean palladium; another cause is the more complex shape of the Pd$_{49}$ island on the PdH(100) surface. Figure 3b shows that edge atoms of the island are pushed up, and the island assumes a hat-like shape. The island is under a high tensile stress, which increases from the edges to the center of the island and can lead to the breaking of large Pd islands on the palladium hydride surface.

In Fig. 4, we present the results for the size-dependent mesoscopic mismatch of single-layer square islands on Pd(100) and PdH(100) surfaces. We can see that the mesoscopic mismatch exists for both heterogenous Pd/PdH(100) and homogenous Pd/Pd(100) systems, but in the case of Pd/PdH(100), the effect of the mesoscopic mismatch is greater because of the existence of a macroscopic misfit between palladium and palladium hydride. As the size of the island increases, the effect of edge atoms becomes less important and the average relative Pd–Pd bond length r/r_0 approaches 1. Because the Pd–Pd bonds are significantly stronger then Pd–H bonds, we suppose that the role of hydrogen in the increasing mesoscopic mismatch is reduced to the swelling of the palladium matrix and to an increase in the lattice constant. The decrease of the average bond
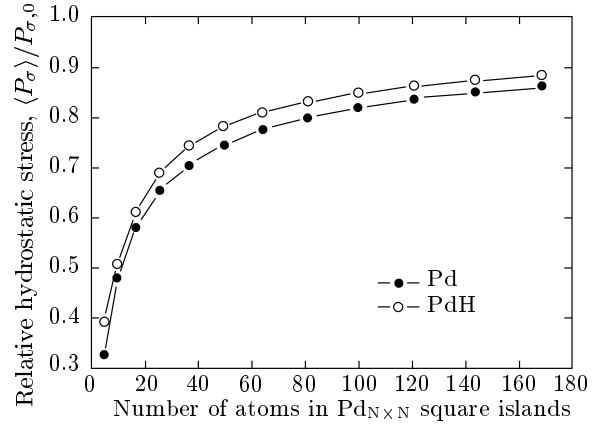
length in the islands is associated with in-plane displacements of the edge atoms toward the center of the island, but relaxation also leads to a decrease in the average height of islands (the distance between the plane of the island and the plane of the topmost Pd layer). We find that the average height of an island decreases with decreasing its size and is almost independent of the concentration of hydrogen in the substrate; the discrepancy between average heights for the Pd$_4$ island and the Pd layer is ≈ 0.1 Å. A more interesting result is the size dependence of the average relative hydrostatic stress of palladium islands presented in Fig. 5. We can see that the curves for Pd(100) and PdH(100) surfaces are very close to each other. Therefore, the relative hydrostatic stress in the palladium islands does not depend on the concentration of hydrogen in the substrate. Hence, the dependence presented in Fig. 5 allows predicting the average hydrostatic stress for every square Pd island on a PdH$_x$(100) surface ($x \in [0,1]$) using only one parameter, the hydrostatic stress of the Pd monolayer. The value of the hydrostatic stress of the Pd monolayer on the PdH$_x$(100) surface lies in the range from 0.21 eV/Å^3 (for clean Pd) to 0.63 eV/Å^3 (for PdH).

We now return to the question about the shape of palladium islands. In Fig. 6, we compare the shapes of small square palladium islands on Pd(100) and PdH(100) surfaces. All Pd islands on the Pd(100) surface presented in Fig. 6a have a tent-like shape. An analogous result has been obtained for hexagonal Cu
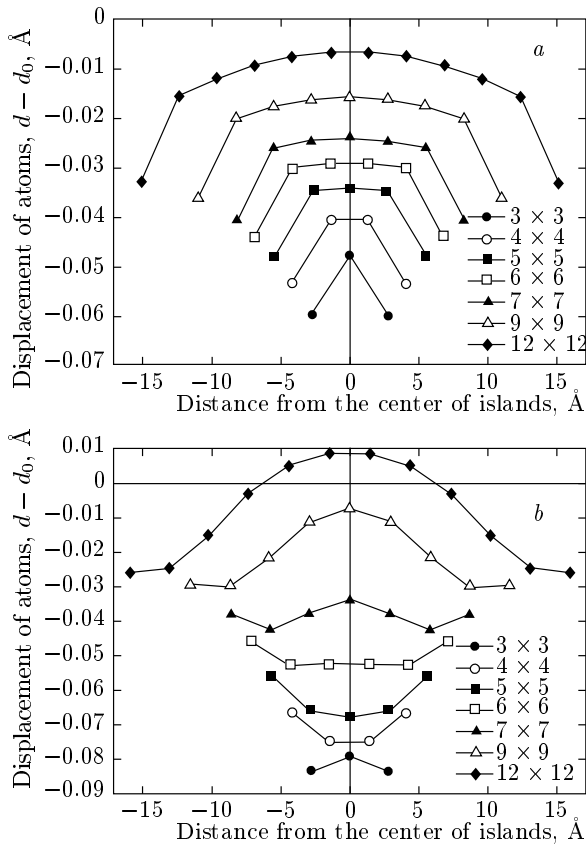
Fig. 6. The vertical displacement $d - d_0$ of Pd atoms in the Pd_9, Pd_{16}, Pd_{25}, Pd_{36}, Pd_{49}, Pd_{81}, and Pd_{144} islands in the $\langle 110 \rangle$ direction. (a) the case of a Pd(100) substrate, (b) the case of a PdH(100) substrate. The interlayer distance $d_0 = 1.91\,\text{Å}$ is the same in both cases
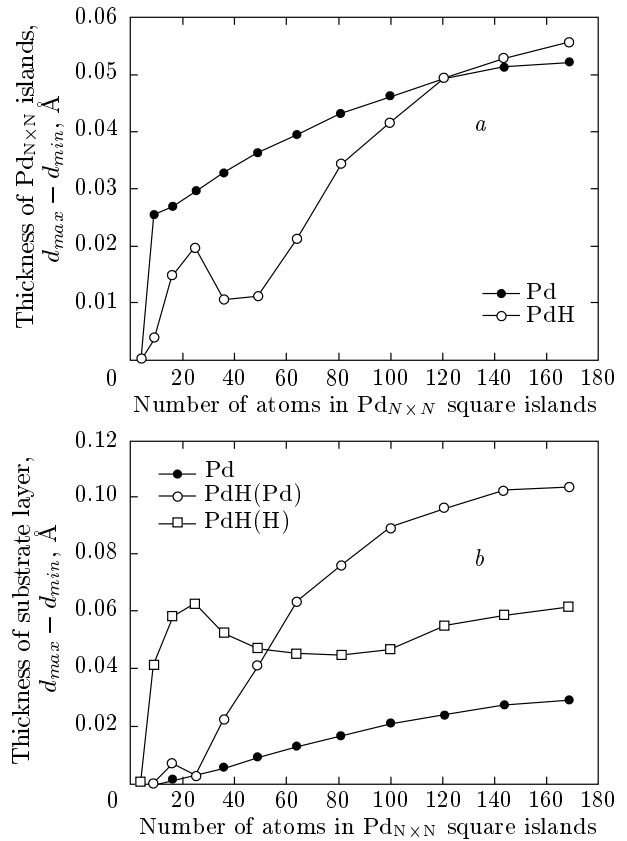

Fig. 7. The thickness $d_{max} - d_{min}$ of (a) palladium islands on Pd(100) and PdH(100) surfaces and (b) the topmost substrate layers under the island. d_{max} and d_{min} are maximal and minimal vertical coordinates of Pd (or H) atoms in the islands or in the substrate layers

island on the Cu(111) surface [13]. Apparently, the tent-like shape of islands is general for every homogenous fcc metal system. The vertical distance between the central Pd atoms in islands and the atoms of the underlying substrate layer monotonically approaches the interlayer distance $d_0 = 1.91\,\text{Å}$. The thickness of islands also has a monotonic dependence on their size (see Fig. 7a). Figure 6b shows that the shapes of Pd islands are more complicated: the small Pd_9 and large Pd_N ($N > 100$) islands have a tent-like shape, the Pd_{16} and Pd_{25} islands have a plate-like shape, and the middle-size Pd_N ($36 \le N \le 81$) islands have an intermediate hat-like shape. This complex size dependence leads to a nonmonotonic increase in the thickness of Pd islands on the PdH(100) surface as the size of islands increases. The vertical distance d between central Pd atoms in the islands and Pd atoms in the underlying substrate layer also has a nonmonotonic size dependence: d increases

for islands from Pd_4 to Pd_{225} and becomes greater than d_0, but then d decreases and approaches d_0 from above.

To understand the origin of the size dependence of shape of Pd islands on the PdH(100) surface, we have calculated the thicknesses of the topmost Pd layer of the Pd(100) surface and the thickness of Pd and H layers of the PdH(100) surface under the Pd islands (Fig. 7b). We can see a monotonic size dependence of the thickness of palladium substrate under the islands on the Pd(100) surface and an almost monotonic size dependence of the thickness of the Pd layer under the islands on the PdH(100) surface. At the same time, the size dependence of the H layer thickness is strongly nonmonotonic; extremums of this curve correlate with modification of the shape of islands. Consequently, the shape of Pd islands on a palladium hydride surface is associated mainly with the Pd–H interaction.

4. CONCLUSION

In summary, we have presented our results obtained for Pd/Pd(100) and Pd/PdH(100) systems. In the presence of impurity atoms in the substrate, the strain and stress inhomogeneities of the topmost substrate layer under islands are increased mainly because of the appearance of a macroscopic misfit between the impure and clean metal. The relative hydrostatic stress in the islands does not depend on the concentration of impurity atoms in the substrate, and it is possible to predict the average hydrostatic stress for islands using only one parameter, the hydrostatic stress of a monolayer. Finally, we can assume that the shape of Pd islands on Pd(100) and PdH(100) surfaces depends only on the peculiarities of the interatomic interaction and does not depend on the macroscopic misfit between the substrate and sputtered metal.

REFERENCES

1. M. Giesen, G. Schulze Icking-Konert, and H. Ibach, Phys. Rev. Lett. **80**, 552 (1998).

2. J. Fassbender, U. May, B. Schirmer et al., Phys. Rev. Lett. **75**, 4476 (1995).

3. A. Gölzhäuser and G. Ehrlich, Phys. Rev. Lett. **77**, 1334 (1996).

4. S. C. Wang and G. Ehrlich, Phys. Rev. Lett. **70**, 41 (1993).

5. C. G. Zimmermann, M. Yeadon, K. Nordlund et al., Phys. Rev. Lett. **83**, 1163 (1999).

6. S. Pick, V. S. Stepanyuk, A. L. Klavsyuk et al., Phys. Rev. B **70**, 224419 (2004).

7. D. Sekiba, Y. Yoshimoto, K. Nakatsuji et al., Phys. Rev. B **75**, 115404 (2007).

8. D. Sander, C. Schmidthals, A. Enders, and J. Kirschner, Phys. Rev. B **57**, 1406 (1998).

9. A. Grossmann, W. Erley, J. B. Hannon, and H. Ibach, Phys. Rev. Lett. **77**, 127 (1996).

10. J. Hafner and D. Spišák, Phys. Rev. B **76**, 094420 (2007).

11. S. A. Chaparro, Y. Zhang, and J. Drucker, Appl. Phys. Lett. **76**, 3534 (2000).

12. V. S. Stepanyuk, D. I. Bazhanov, A. N. Baranov et al., Phys. Rev. B **62**, 15398 (2000).

13. O. V. Lysenko, V. S. Stepanyuk, W. Hergert, and J. Kirschner, Phys. Rev. Lett. **89**, 126102 (2002).

14. C. Gilmore, J. Sprague, J. Eridon, and V. Provenjano, Surf. Sci. **218**, 26 (1989).

15. C. Massobrio and P. Blandin, Phys. Rev. B **47**, 13687 (1993).

16. T. O. Menteş, N. Stojić, N. Binggeli et al., Phys. Rev. B **77**, 155414 (2008).

17. N. N. Negulyaev, V. S. Stepanyuk, L. Niebergall et al., Phys. Rev. B **79**, 195411 (2009).

18. O. Mironets, H. L. Meyerheim, C. Tusche et al., Phys. Rev. Lett. **100**, 096103 (2008).

19. O. Mironets, H. L. Meyerheim, C. Tusche et al., Phys. Rev. B **79**, 035406 (2009).

20. W. Zhong, Y. S. Li, and D. Tománek, Phys. Rev. B **44**, 13053 (1991).

21. D. Tománek, S. G. Louie, and C. T. Chan, Phys. Rev. Lett. **57**, 2594 (1986).

22. D. Tománek, Z. Sun, and S. G. Louie, Phys. Rev. B **43**, 4699 (1991).

23. A. Lahee, J. Toennies, and C. Well, Surf. Sci. **191**, 529 (1987).

24. M. Skottke, R. J. Behm, G. Ertl et al., J. Chem. Phys. **87**, 6191 (1987).

25. S. C. Jung and M. H. Kang, Phys. Rev. B **72**, 205419 (2005).

26. F. Cleri and V. Rosato, Phys. Rev. B **48**, 22 (1993).

27. G. Kresse and J. Hafner, Phys. Rev. B **48**, 13115 (1993).

28. G. Kresse and J. Furthmuller, Comp. Mater. Sci. **6**, 15 (1996).

29. G. Kresse and D. Joubert, Phys. Rev. B **59**, 1758 (1999).

30. W. Yu and A. Madhukar, Phys. Rev. Lett. **79**, 905 (1997).